RAA 2014 Vol. **14** No. **12**, 1654–1663 doi: 10.1088/1674–4527/14/12/013
http://www.raa-journal.org *http://www.iop.org/journals/raa*

Research in Astronomy and Astrophysics

Development and calibration of the Moon-based EUV camera for Chang'e-3

Bo Chen, Ke-Fei Song, Zhao-Hui Li, Qing-Wen Wu, Qi-Liang Ni, Xiao-Dong Wang, Jin-Jiang Xie, Shi-Jie Liu, Ling-Ping He, Fei He, Xiao-Guang Wang, Bin Chen, Hong-Ji Zhang, Xiao-Dong Wang, Hai-Feng Wang, Xin Zheng, Shu-Lin E, Yong-Cheng Wang, Tao Yu, Liang Sun, Jin-Ling Wang, Zhi Wang, Liang Yang, Qing-Long Hu, Ke Qiao, Zhong-Su Wang, Xian-Wei Yang, Hai-Ming Bao, Wen-Guang Liu, Zhe Li, Ya Chen, Yang Gao, Hui Sun and Wen-Chang Chen

Changchun Institute of Optics, Fine Mechanics and Physics, Chinese Academy of Sciences, Changchun, 130033, China; *chenb@ciomp.ac.cn*

Received 2014 July 27; accepted 2014 September 27

Abstract The process of development and calibration for the first Moon-based extreme ultraviolet (EUV) camera to observe Earth's plasmasphere is introduced and the design, test and calibration results are presented. The EUV camera is composed of a multilayer film mirror, a thin film filter, a photon-counting imaging detector, a mechanism that can adjust the direction in two dimensions, a protective cover, an electronic unit and a thermal control unit. The center wavelength of the EUV camera is 30.2 nm with a bandwidth of 4.6 nm. The field of view is 14.7° with an angular resolution of 0.08°, and the sensitivity of the camera is 0.11 count s^{-1} Rayleigh^{-1}. The geometric calibration, the absolute photometric calibration and the relative photometric calibration are carried out under different temperatures before launch to obtain a matrix that can correct geometric distortion and a matrix for relative photometric correction, which are used for in-orbit correction of the images to ensure their accuracy.

Key words: Chang'e-3 — EUV camera: development: calibration — Earth's plasmasphere — lunar exploration

1 INTRODUCTION

1.1 International Developments

Earth's plasmasphere is a torus-shaped region with dense, low energy plasma located above the ionosphere which extends to 5∼6 $R_\oplus$ (Earth radii, 1 $R_\oplus = 6371$ km). All the charged particles in the plasmasphere are trapped on geomagnetic field lines (Lemaire & Gringauz 1998). The plasmaspheric He^+ ions resonantly scatter the extreme ultraviolet (EUV) radiation of sunlight at 30.4 nm with intensity that is proportional to the column density along the line of sight (Meier 1991). Since He^+ ions are the second most abundant component in the plasmasphere (Craven et al. 1997), their distribution

can reflect the global structure of the plasmasphere. The facts that the magnetosphere is optically thin to 30.4 nm emission and the interplanetary background is extremely low make Moon-based EUV plasmaspheric imaging suitable and the imaging process simple. Thus, imaging at 30.4 nm is the best choice for monitoring the global plasmasphere and the EUV images are intuitively suitable for research on the dynamics and global structures of the plasmasphere during storms/substorms, as well as for space weather monitoring and forecasting (He et al. 2013).

The optical remote sensing of the plasmasphere began in the 1970s, starting with low-orbit photometry measurements (Weller & Meier 1974) and continuing through partial imaging by instruments in high orbits (Nakamura et al. 1999), and finally an imager with a large field of view (FoV) to image the global plasmasphere (Sandel et al. 2000). The EUV Imager (Sandel et al. 2000) onboard the IMAGE mission was launched in May 2000 and obtained many important scientific discoveries during its lifetime of nearly five years. The IMAGE mission was operated in a polar orbit around Earth with a perigee of $\sim$1000 km and an apogee of $\sim$42 000 km. The FoV of the EUV imager was composed of three identical sub-FoVs of 30°. With that instrument, the plasmasphere could only be completely imaged in the apogean region around the north pole. The EUV imager was mounted on a spinning platform and the IMAGE mission was operated in a polar orbit with limited FoV and only half (or less) of the duty circle could view the whole plasmasphere; therefore, the plasmasphere could not be continuously imaged.

The EUV Camera (EUVC) developed at Changchun Institute of Optics, Fine Mechanics and Physics, Chinese Academy of Sciences landed on the lunar surface as part of the Chang'e 3 (CE-3) lunar lander (Ip et al. 2014; He et al. 2010) and has taken photos of Earth's plasmasphere from a perspective on the side during the past half year.

1.2 Scientific Goals

During its one year lifetime, EUVC took a number of photos of the plasmasphere in order to achieve the following scientific goals.

(1) Image Earth's plasmasphere at 30.4 nm from the perspective of the side at different positions along the orbit of the Moon to investigate three-dimensional structures in the plasmasphere.
(2) Continuously image the plasmasphere over a relatively long duration to monitor evolution of the plasmaspheric density and structure with geomagnetic activity.

1.3 Technical Requirements

In order to achieve its scientific goals, the EUVC should have a high response at 30.4 nm and filter 58.4 nm emission from the ionosphere. In addition, it should have a large enough FoV to cover the entire plasmasphere and have a good spatial resolution that can identify plasmaspheric structures. The specifications for the EUVC are listed in Table 1.

Table 1 Specifications for the EUVC

Parameter	Value
Central wavelength (nm)	30.4 ± 0.5
Spectral bandwidth (nm)	$\leq$5.0
Field of view (°)	15.00 ± 0.75
Angular resolution (°)	$\leq$0.10
Exposure time (min)	2, 10 or 20
Dynamic range (Rayleigh)	0.1$\sim$10.0
Sensitivity (count s^{-1} $Rayleigh^{-1}$)	$\geq$0.10
Sensitivity ratio at 30.4 nm and 58.4 nm	$\geq$70.0

The arrangement of this paper is as follows. Section 2 gives the overview of the EUVC and the general test results, Section 3 provides the detailed design of the EUVC, Section 4 details the calibration of the EUVC, the first image and image processing will be described in Section 5, and a summary will be given in Section 6.

2 OVERVIEW OF EUVC AND GENERAL TEST RESULTS

The EUVC, designed for the lunar environment, is mainly composed of a main structure and an electronics box, with the main structure mounted outside the instrumental module on the top of the lunar lander and the electronics box inside the module. The main structure of EUVC is composed of a multilayer film mirror, a thin film filter, a preamplifier, a sunshade and a protective cover. The rotation mechanism is composed of a pitch control mechanism, an azimuth control mechanism and corresponding mechanical positioning units. The electronic system is composed of a wave shaping circuit, a high speed A/D conversion unit, EUVC control unit, stepper motor driving unit, FPGA, and a temperature acquisition and processing unit. A schematic diagram of the electronic system for EUVC is shown in Figure 1 and a photo of the EUVC is presented in Figure 2.

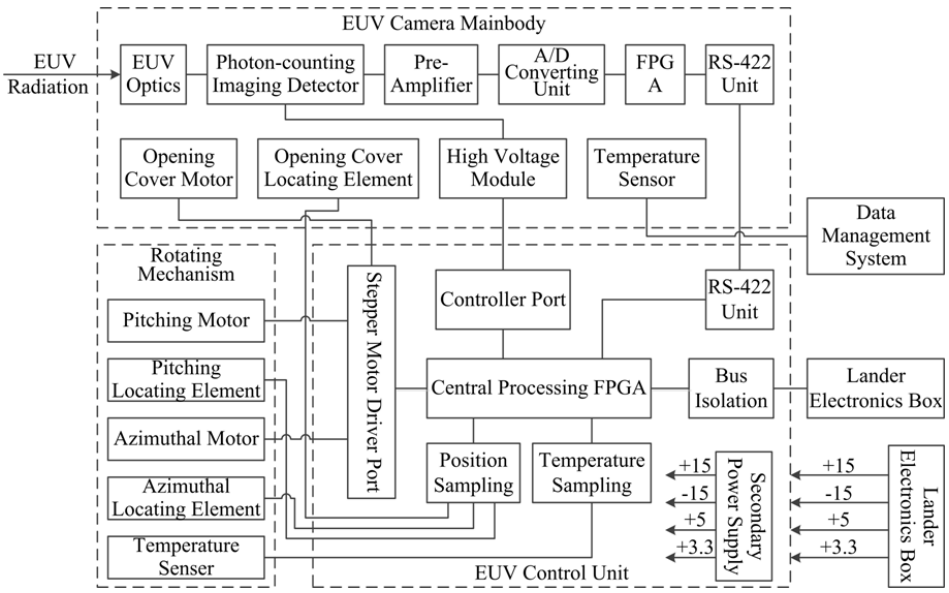

Fig. 1 Schematic diagram of the electronic system for the EUVC.

Before launch, the performance of the EUVC was tested in detail and the results are listed in Table 2. Table 2 indicates that the performance of EUVC satisfies the technical requirements and fulfills the requirements of imaging the plasmasphere on the lunar surface over a long duration.

3 DESIGN OF EUVC

3.1 Optical Design

Since no material that transmits in optical is suitable for the EUV wavelength range, the EUVC should implement a reflective optical system (Chen & He 2011), among which both grazing incidence designs and normal incidence designs are applicable. Commonly used grazing incidence

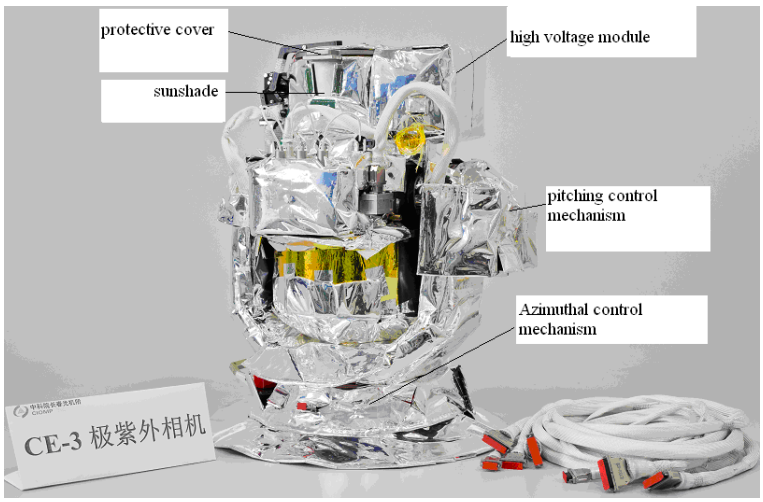

Fig. 2 Photo of the EUVC.

Table 2 Test Results of EUVC

Parameter	Test results
Center wavelength (nm)	30.2
Bandwidth (nm)	4.6
Sensitivity ratio at 30.4 nm and 58.4 nm	79.2
FoV (°)	14.7
Angular resolution (°)	0.08
Exposure time (min)	2,10, 20
Dynamic scope (Rayleigh)	0.1∼10
Sensitivity (count s^{-1} $Rayleigh^{-1}$)	0.11

designs include Wolter type and KB type, both of which have the property of a small FoV and large volume which are not suitable for the EUVC. Normal incidence designs include Cassegrain and Schwarzchild, both of which can achieve high resolution. However, the Cassegrain design can only achieve high resolution in a small FoV and needs two mirrors. The Schwarzchild design also needs two mirrors but its volume is relatively large. So, both Cassegrain and Schwarzchild designs are also not applicable for EUVC. Finally, a design with a single spherical mirror and a spherical detector is chosen, as shown in Figure 3. This layout has the advantages of a small volume, large FoV and high efficiency in energy transfer which are suitable for application in the environment on the lunar surface.

Since the emissions from the plasmasphere are very weak, between 0.1∼10 Rayleigh, a photon-counting imaging detector with high sensitivity is needed. The parameters of the detector are spatial resolution of 0.20 mm, effective diameter of 40 mm, radius of curvature of the microchannel plate (MCP) of 150 mm and dark counting rate of 1 count s^{-1} cm^{-2}. The structure of the detector is shown in Figure 4, in which 1 is the supporting assembly for the MCP, 2 is the position sensitive anode, 3 is the fixing and supporting assembly for the anode, 4 is the electronic connector, 5 is the baseplate for installation, 6 is the insulating layer, and 7 is the supporting frame.

The parameters of the optimized optical system are listed in Table 3. A diagram showing the optical path and the spot diagrams are presented in Figure 3 and Figure 5 respectively. The plasmaspheric EUV emissions entering into the system through the entrance pupil are reflected to the focal plane by the spherical multilayer film mirror, and then the EUV photons are transformed into photoelectric signals by a photon counting imaging detector. In Figure 3, the blue, green, red and

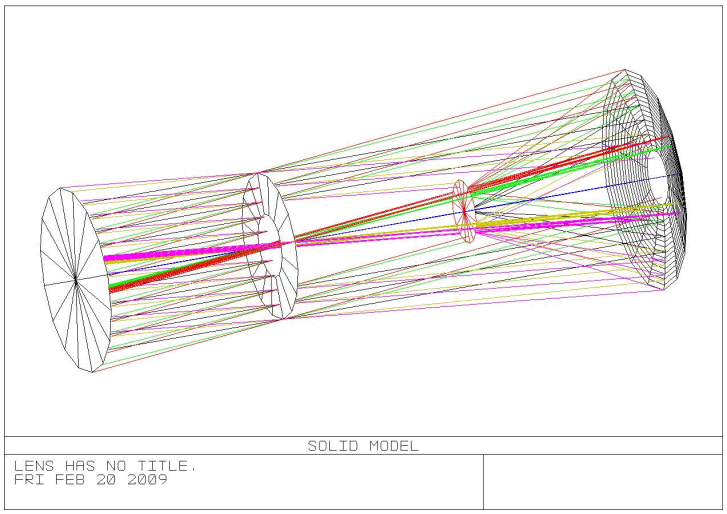

Fig. 3 Diagram showing the optical path of the EUVC.

Table 3 Optimized Optical Parameters of the EUVC

Parameter	Value
Wavelength (nm)	30.4
FoV (°)	15 (Circular)
Angular resolution (°)	0.08
Diameter of the mirror (mm)	187.1
Radius of curvature of the mirror (mm)	300.0
Effective diameter of the detector (mm)	Φ40.0
Focal length (mm)	150.0

yellow lines represent the $0°$, $3°$, $5°$ and $7.5°$ FoVs, respectively. The radii of the spot diagrams in Figure 5 are 0.204 mm ($0°$), 0.203 mm ($3°$), 0.202 mm ($5°$) and 0.205 mm ($7.5°$). The detector has a spatial resolution of 0.2 mm, effective diameter of 40 mm and dark count rate of 1 count s^{-1} cm^{-2}. Therefore, the calculated angular resolution of EUVC is $0.08°$, satisfying the requirements of the EUVC.

3.2 Operating Wavelength

The ionosphere, located under the plasmasphere, contains a number of helium atoms which can strongly scatter sunlight at 58.4 nm. The average intensity of ionospheric 58.4 nm emission is approximately 500 Rayleigh, much higher than the plasmaspheric 30.4 nm emission of $\sim$10 Rayleigh (He et al. 2013). Since the ionosphere is always in the FoV of EUVC, the 58.4 nm emissions that enter the EUVC can reduce the signal-to-noise ratio of the EUV images. Also, the strong 58.4 nm emissions may cause saturation of the detector. So, the 58.4 nm emissions must be filtered to effectively image the 30.4 nm emissions from the plasmasphere.

In order to filter the 58.4 nm emissions, we have adopted the following methods. First, an EUV multilayer film mirror with a bandwidth of 4.6 nm is used as a narrowband filter to enhance the reflectivity at 30.4 nm and reduce the reflectivity at other wavelengths. Second, a thin film filter is used to filter the transmission with wavelength greater than 50 nm. Third, the quantum efficiency of the detector is very low around 50 nm. Finally, the ratio of detective quantum efficiency for EUVC

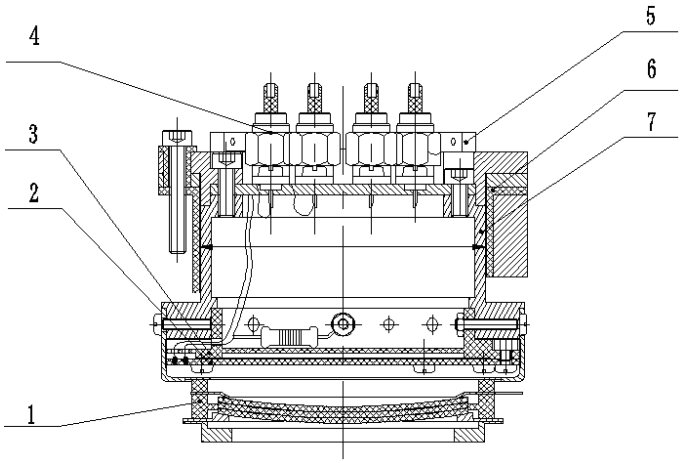

Fig. 4 Structure of the detector.

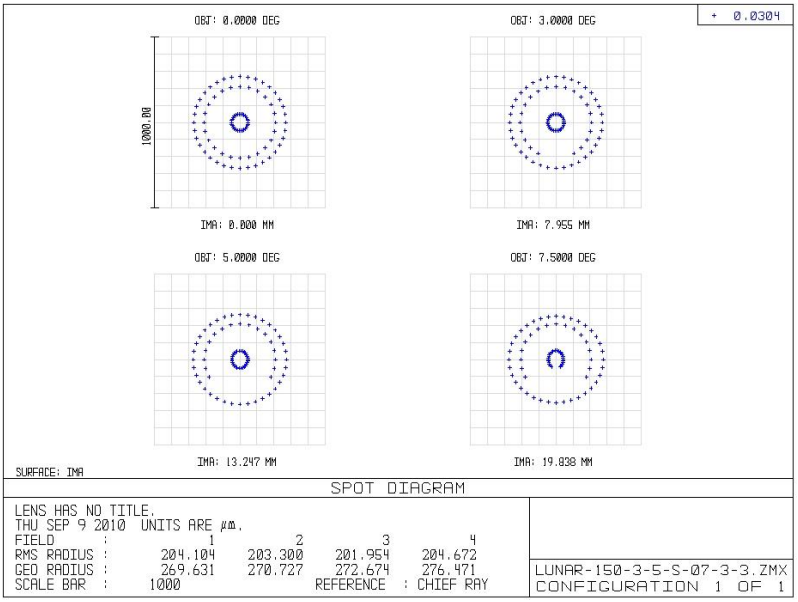

Fig. 5 Spot diagrams of the EUVC.

at 30.4 nm is 79.2 times higher than that at 58.4 nm. The 58.4 nm radiation and others out of the operating wavelengths are efficiently filtered.

3.3 Sensitivity of EUVC

The sensitivity of the EUVC is determined by the area of the entrance pupil, the solid angle of a spatial resolution element, the reflectivity of the mirror, the transmission of the filter and the quantum efficiency of the detector. The sensitivity S can be calculated by the formula

$$S = A \times \omega \times \varepsilon \times \tau \times \rho \times \frac{10^6}{4\pi}\,, \tag{1}$$

where ω is the solid angle of a spatial resolution element, τ is the transmission of the filter, ρ is the reflectivity of the multilayer film mirror, ε is the quantum efficiency of the detector and A is the area of the entrance pupil. According to the tests, $\rho = 0.187$, $\tau = 0.209$, $\varepsilon = 0.148$, $\omega = 3.1 \times 10^{-6}$ sr and $A = 80.6\,\mathrm{cm}^2$. Using the above values, we find $S = 0.11$ count s^{-1} $\mathrm{Rayleigh}^{-1}$, which satisfies the requirement of the EUVC.

3.4 Design of the Rotation Mechanism

Because the EUVC is mounted outside the instrumental module on the top of the lunar lander, a mechanism for adjusting the direction is needed to change the direction of the axis of the FoV to track Earth. During launch, the axis of the FoV is perpendicular to the the module plate. After landing, the axis of the FoV should be adjusted to point to the center of Earth. Under normal operation, a two-dimensional adjustment is necessary for real-time tracking of the center of the Earth since the Moon has a latitudinal and a longitudinal drift during its rotation around Earth.

The two-dimensional mechanism is composed of a U-shaped support, an azimuthal rotation mechanism and a latitudinal rotation mechanism. The rotations in both dimensions are driven by a stepper motor. According to the location of the landing site, the azimuthal adjustment range is $92^\circ \sim 192^\circ$ and the latitudinal adjustment range is $15^\circ \sim 90^\circ$, with an adjustment accuracy of 0.1°. During operation, the axis of the FoV is adjusted in real time according to telemetry from the probe to ensure that Earth's center is always located at the center of the FoV and to image the plasmasphere completely. Five months of successful operation on the lunar surface indicates that the rotation mechanism satisfies the requirements.

4 CALIBRATION OF EUVC

4.1 Geometric Calibration

Both the EUV optics and the detector on the EUVC have geometrical distortions which must be corrected. The distortion in the detector, which is greater than that in the optical system, can be corrected by optimizing the position decoding formula of the anode. The correction parameters are obtained during ground tests and can be applied to the EUVC when it is on the lunar surface.

The overall distortion of the EUVC is determined by ground calibration with polynomial functions

$$\begin{cases} x = a(x_\mathrm{d}, y_\mathrm{d}) = \sum\limits_{i=0}^{N} \sum\limits_{j=0}^{N} P_{i,j} x_\mathrm{d}^i y_\mathrm{d}^j \,, \\ y = b(x_\mathrm{d}, y_\mathrm{d}) = \sum\limits_{i=0}^{N} \sum\limits_{j=0}^{N} Q_{i,j} x_\mathrm{d}^i y_\mathrm{d}^j \,, \end{cases} \tag{2}$$

where (x, y) corresponds to the coordinate in the undistorted image, $(x_\mathrm{d}, y_\mathrm{d})$ corresponds to the coordinate in the distorted image, P and Q are the parameters to be determined and N equals 3. P and Q are determined by imaging point sources which are stars. Distorted images of these points which are stars are acquired with the displacement of the points being 1° in both the latitudinal and azimuthal directions. The coordinates of the distorted and undistorted image are used to solve the polynomial parameters as listed in Table 4. The residual distortions at different temperatures are listed in Table 5.

4.2 Photometric Calibration

Photometric calibration includes absolute calibration and relative calibration. Details are as follows.

Table 4 Distortion Correction Parameters

Primary preamplifier P_{ji}			0	1	2	3
0	Primary preamplifier	P	1.48568×10^{2}	7.82340×10^{-2}	-1.64382×10^{-4}	1.06927×10^{-7}
		Q	7.09858×10^{2}	-1.22060×10^{0}	2.31262×10^{-3}	-8.56862×10^{-7}
	Backup preamplifier	P	1.47389×10^{2}	7.76131×10^{-2}	-1.63077×10^{-4}	1.06078×10^{-7}
		Q	7.06327×10^{2}	-1.21453×10^{0}	2.30111×10^{-3}	-8.52599×10^{-7}
1	Primary preamplifier	P	5.05771×10^{-1}	-1.47789×10^{-3}	2.06959×10^{-6}	-8.85995×10^{-10}
		Q	-2.20706×10^{0}	6.94997×10^{-3}	-7.11524×10^{-6}	2.55511×10^{-9}
	Backup preamplifier	P	5.01757×10^{-1}	-1.46616×10^{-3}	2.05317×10^{-6}	-8.78963×10^{-10}
		Q	-2.19608×10^{0}	6.91539×10^{-3}	-7.07984×10^{-6}	2.54240×10^{-9}
2	Primary preamplifier	P	6.52983×10^{-4}	2.24512×10^{-6}	-3.19262×10^{-9}	1.33392×10^{-12}
		Q	2.48538×10^{-3}	-8.42840×10^{-6}	9.10806×10^{-9}	-3.31964×10^{-12}
	Backup preamplifier	P	6.47801×10^{-4}	2.22730×10^{-6}	-3.16728×10^{-9}	1.32333×10^{-12}
		Q	2.47301×10^{-3}	-8.38647×10^{-6}	9.06275×10^{-9}	-3.30312×10^{-12}
3	Primary preamplifier	P	-3.72497×10^{-7}	-6.80674×10^{-10}	1.17403×10^{-12}	-5.42679×10^{-16}
		Q	-8.58296×10^{-7}	3.16782×10^{-9}	-3.58877×10^{-12}	1.31266×10^{-15}
	Backup preamplifier	P	-3.69541×10^{-7}	-6.75272×10^{-10}	1.16471×10^{-12}	-5.38372×10^{-16}
		Q	-8.54025×10^{-7}	3.15206×10^{-9}	-3.57091×10^{-12}	1.30613×10^{-15}

Table 5 Residual Distortions in the EUVC

Temperature	–25℃	25℃	75℃
Max. residual distortion of the primary preamplifier	1.0%	1.2%	1.8%
Max. residual distortion of the backup preamplifier	1.4%	1.2%	1.7%

Table 6 Responses of the EUVC at Different Temperatures

Temperature	Sensitivities with Primary preamplifier (count s^{-1} $Rayleigh^{-1}$)	Sensitivities with Backup preamplifier (count s^{-1} $Rayleigh^{-1}$)
–25℃	0.10	0.10
25℃	0.11	0.11
75℃	0.14	0.14

4.2.1 Absolute photometric calibration

The goal of absolute calibration is to determine the relationship between the responses of the EUVC and the intensity of the target. The response function of the EUVC to a target is

$$I = \frac{I_{\mathrm{p}}}{t \cdot S}\,, \tag{3}$$

where I_{p} is the pixel value, t with a value of 600 s is the exposure time and S is the sensitivity of the EUVC. According to the test in Section 3.3, the sensitivities of the EUVC at different temperatures are listed in Table 6.

4.2.2 Relative photometric calibration

The goal of the relative photometric calibration or the flat field calibration is to determine the response uniformity of the active surface in the EUVC detector. The response uniformity of the EUVC depends on the detector response and the vignette of the EUV optics. The uniformity is calibrated after assembly of the EUVC. The responses of the EUVC in different FoVs are measured at intervals

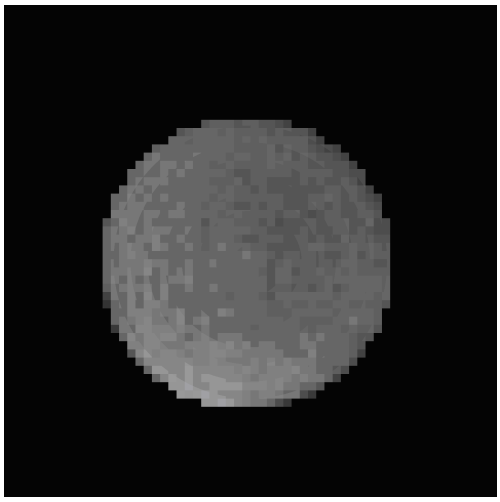

Fig. 6 The relative photometric correction matrix for the EUVC.

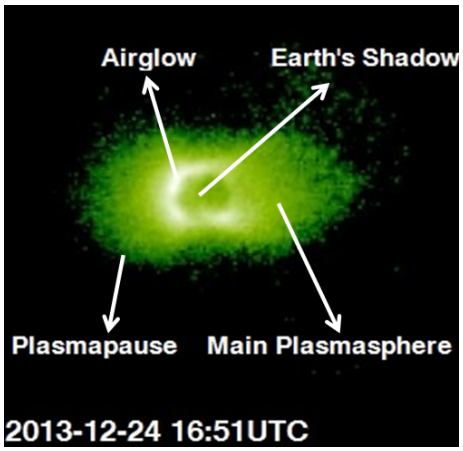

Fig. 7 Image of the plasmasphere taken at 16:51 UT on 2013 December 24.

of 1°. During the calibration, the same EUV source is applied under the same working pressure and current, so that the intensity of EUV radiation stays the same. The calibration result is shown in Figure 6 and can be used to apply flat field correction to images of the plasmasphere. The results of the calibrations show that values are uniform within 15.8%. The results of observations from the EUVC on the lunar surface are modified by the uniformly corrected data so that the real distributions of the plasmasphere are obtained.

5 FIRST IMAGE AND IMAGE PROCESSING

The EUVC landed on the lunar surface on 2013 December 12 and obtained the first global image of the plasmasphere from the Moon. After an image of the plasmasphere was acquired, the EUVC was rotated away from the Earth to take a dark image of the background. Then the background was removed from the image of the plasmasphere. The result is shown in Figure 7. The plasmasphere, plasmapause, airglow and the Earth's shadow can be clearly seen in the image. During its long term

observations, data from the EUVC will provide useful images for researchers to investigate how the plasmasphere responds to solar activities.

6 SUMMARY

The development and calibration of the EUVC have been done and all the performance parameters satisfy the scientific requirements. The EUVC has successfully landed on the lunar surface and has obtained many images of the plasmasphere in EUV. Both ground and in-orbit tests indicate that the performance of the EUVC has achieved the design requirements and satisfies the needs of scientific research. The FoV of the EUVC is 14.7°, which can cover the overall plasmasphere; the angular resolution is 0.08°, which can clearly resolve plasmaspheric structures; the working wavelength is 30.2 nm with a bandwidth of 4.6 nm and the radiation with wavelength longer than 58.4 nm, which is UV and visible light, is strongly filtered, ensuring effective imaging of the plasmasphere; the dynamic range is $0.1 \sim 10$ Rayleigh which covers the whole possible range of emissions from the plasmasphere and clearly resolves the plasmapause.

References

Chen, B., & He, F. 2011, Optics and Precision Engineering, 19, 2057 (in Chinese)
Craven, P. D., Gallagher, D. L., & Comfort, R. H. 1997, J. Geophys. Res., 102, 2279
He, F., Chen, B., & Zhang, X.-X. 2010, Optics and Precision Engineering, 18, 2564 (in Chinese)
He, F., Zhang, X.-X., Chen, B., Fok, M.-C., & Zou, Y.-L. 2013, Journal of Geophysical Research (Space Physics), 118, 7085
Ip, W.-H., Yan, J., Li, C.-L., & Ouyang, Z.-Y., 2014, RAA (Research in Astronomy and Astrophysics), 14, 1511
Lemaire, J. F., & Gringauz, K. I. 1998, The Earth's Plasmasphere (Cambridge: Cambridge Univ. Press)
Meier, R. R. 1991, Space Sci. Rev., 58, 1
Nakamura, M., Yamashita, K., Yoshikawa, I., et al. 1999, Earth, Planets, and Space, 51, 61
Sandel, B. R., Broadfoot, A. L., Curtis, C. C., et al. 2000, Space Sci. Rev., 91, 197
Weller, C. S., & Meier, R. R. 1974, J. Geophys. Res., 79, 1572